International Journal of Automotive Technology, Vol. 7 No. 3, pp. 261–267 (2006)

1229-9138/2006/027-04

INVESTIGATION OF SOOT OXIDATION CHARACTERISTICS IN A SIMULATED DIESEL PARTICULATE FILTER

H.-S. LEE[1)] and K. M. CHUN[2)*]

[1)]Graduate School of Mechanical Engineering, Yonsei University, Seoul 133-768, Korea
[2)]Department of Mechanical Engineering, Yonsei University, Seoul 133-768, Korea

(Received 27 December 2005; Revised 8 November 2005)

ABSTRACT–Understanding the mechanism of carbon oxidation is important for the successful modeling of diesel particulate filter regeneration. Carbon oxidation characteristics were investigated by temperature programmed oxidation (TPO) method as well as constant temperature oxidation (CTO) with a flow reactor including porous bed. The activation energy of carbon oxidation was increasing with temperature and had two different constant values in the early and the later stage of the oxidation process respectively in TPO experiment. Kinetic constants were derived and the reaction mechanisms were assumed from the experimental results and a simple reaction scheme was proposed, which approximately predicted the overall oxidation process in TPO as well as CTO.

KEY WORDS : Carbon oxidation, Constant temperature oxidation, Temperature programmed oxidation, Activation energy, Reaction mechanism, DPF, Diesel engine

1. INTRODUCTION

Diesel engine exhaust is one of the major sources of atmospheric pollution. Emission regulations are becoming increasingly stringent and demand low emission diesel technologies. Diesel particulate filter (DPF) systems are reliable solutions for reducing soot from diesel exhaust.

Though most of the DPFs have enough efficiency over 95% for dry soot in trapping, their regeneration is still quite challenging because the exhaust temperature and the soot emission amount have wide variation between types and driving conditions of diesel light and heavy duty vehicles. Furthermore, the knowledge on oxidation characteristics of diesel soot is not so clear that reliable performance expectation of a DPF system for a vehicle application is yet difficult. The results from researchers have varied in kinetic values and some of them are contradictory. For these reasons, this subject is still on extensive research (Bokova *et al.*, 2004; Haralampous *et al.*, 2004; Stratakis and Stamatelos, 2003; Yezerets *et al.*, 2003; Vincent *et al.*, 2002).

DPF requires heat and oxidant for its regeneration. Major oxidants in diesel application are oxygen and nitrogen dioxide. NO_2 oxidizes soot at lower temperature than O_2. A well known commercial DPF system of CRT (continuous regeneration trap) utilizes NO_2 and its BPT (balance point temperature) is as low as 250°C with required NO_2/soot ratio (Allansson *et al.*, 2002). However, at real driving condition, average exhaust temperature of light duty vehicle such as passenger cars is frequently lower than 200°C, and in such cases the active regeneration with forced temperature rise is required to avoid high backpressure that can cause poor fuel economy and engine stop. Active regeneration utilizes O_2 preferably for its fast reaction. However careful management of the oxidation speed is needed to avoid the uncontrolled regeneration that can cause DPF failure (Dieselnet Technology Guide, 2005).

Investigation procedures of DPF regeneration in a real condition using engine system usually take long time giving only a few determining data. The loading of soot to a certain amount takes at least a few hours or more. In a real system the regeneration of DPF can only be evaluated by the back pressure because it's not possible to measure the CO and CO_2 production from soot oxidation. But the back pressure at DPF is more sensitive to the volume flow rate than the amount of soot loading. Furthermore, the temperature distribution and the soot loading in a DPF are not uniform. For these reasons, a well organized experiment of laboratory scale should be performed for the evaluation of soot oxidation, which can enable the simulation over wide range of temperature, soot loading and oxidation conditions.

*Corresponding author. e-mail: kmchun@yonsei.ac.kr

A number of studies have shown that carbon oxidation has mainly two different reaction steps of adsorption of oxygen onto the carbon surface forming surface oxidation complexes and desorption of them as carbon oxides (Stanmore *et al.*, 2001) and the activation energy changes apparently during oxidation process. It was also shown that the carbon oxidation has lower activation energy of 35–70 kJ/mol in the early stage, and after oxidation of 10–30% of the carbon, activation energy increases up to 140–210 kJ/mol (Haralampous *et al.*, 2004; Jung *et al.*, 2004; Yezerets *et al.*, 2002). These values also varies depending upon the origin of samples; carbon black, activated carbon, diesel soot, graphite, etc. (Clague *et al.*, 1999; Su *et al.*, 2004; Vander Wal *et al.*, 2003). A commercial carbon black is usually selected as a model soot in oxidation experiment for its consistency in oxidation characteristics.

In this work, we established experimental methodology and simulated soot oxidation with carbon black and oxygen. Printex-U, a commercial carbon black was used as model soot.

2. EXPERIMENT

There are two major experimental methods in carbon oxidation experiment. One is thermogravimetric analysis (TGA) and the other is fixed bed reactor analysis. TGA has the advantage of measuring directly the mass of carbon during oxidation process so that the volatile portion of the soot can be also determined. But this method cannot ignore the diffusion effect and must be performed with low gas flow rate (Gilot *et al.*, 1993; Neeft *et al.*, 1996). A flow reactor with a porous bed can simulate a real DPF condition better that has forced gas flow passing through carbon deposit layer. Soot samples are commonly used with inert media such as quartz chips or SiC powder for the better heat dissipation in exothermic reactions. However, with a certain amount of diluents the temperature difference in the reaction area can increase in a temperature programmed oxidation procedure (Yezerets *et al.*, 2002). In this experiment no diluents was used by this reason and no exothermic effect was confirmed. Figure 1 shows the soot deposition on the DPF wall (a) and the sample preparation of one of other researchers (b) and ours (c). Figure 2 shows the experimental system used in this work.

The reactor was made of quartz and has a ceramic fiber filter at the location of 2/3 from the top inlet. The inner diameter of the reactor is 20 mm and was bottle-necked to 14 mm at the reaction bed to minimize the temperature difference to the radial direction. 20 mg of carbon black (Printex-U) was used as soot sample. The carbon sample was deposited onto the filter and a k-type thermocouple was located on the sample bed. The reactor was covered

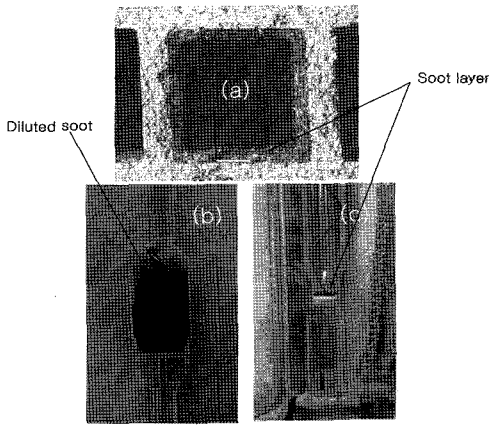

Figure 1. Soot deposit on DPF wall (a), diluted soot sample with quartz chips, (Yezerets *et al.*, 2002) (b), soot sample deposit in this work (c).

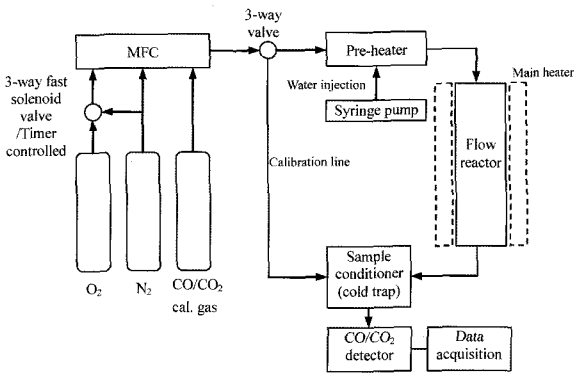

Figure 2. Schematics of the experimental setup.

with an electric heater that can heat the gas flow up to 670°C. The inlet gas was pre-heated with the line heater before the main reactor inlet. Total flow rate was 1 liter per minute and the gas composition was controlled by mass flow controllers. The maximum temperature deviation in the carbon deposition was under 3°C.

CO and CO_2 emissions from carbon oxidation were measured by non-disperse infra-red detector (Teledyne 7500 series). A cold trap was installed before the analyzer for sample conditioning. The temperatures and the analog outputs of the detector were recorded by the data acquisition system (data translation 9805 series). Data were sampled by one set per second.

Oxygen concentration in the feed gas was 10% and controlled by MFC in nitrogen background gas. We used temperature programmed oxidation (TPO) technique as well as constant temperature oxidation (CTO). In TPO procedure, temperature was increased by 3.8°C per minute from the room temperature up to 670°C. Until the temperature at the reaction bed reached 150°C, the feed gas was only nitrogen and oxygen was mixed from that

Table 1. Elemental composition of Printex-U.

	C	H	N	S	O
wt%	93.3	0.6	0.4	< 0.3	3.8

temperature.

In CTO procedure the carbon sample was heated in nitrogen up to the desired temperature, and then oxygen was fed to the gas flow. At the end of each experiment, the remaining amount of soot was completely oxidized by heating up to 670°C, in order to close the carbon balance.

The carbon oxidation rate was calculated from the measured CO and CO_2 concentrations by Equation (1).

Carbon oxidation rate (μg/sec)

$$=\frac{(CO+CO_2)(ppm)\times M_{W,carbon}(g/mol)\times \dot{V}_{total}(l/sec)}{\text{molarvolume (l/mol at std)}} \quad (1)$$

The remaining soot amount is important in determining of kinetic values. Initial soot mass is mainly the sum of elemental carbon and oxygen. However, the total sample amount calculated from CO and CO_2 emissions can evaluate only elemental carbon amount. Table 1 is the elemental composition of Printex-U. The measured total elemental carbon amount from the experiment was 93 ± 2%, which matches well with the elemental analysis result.

3. RESULT AND DISCUSSION

Figure 3 shows a result from the experiment as the temperature increases (TPO). The apparent carbon oxidation started around 350°C. From the measured CO, CO_2 concentrations, the carbon oxidation rate was calculated directly by Equation (1) and the total carbon amount was calculated by integration of the rate. Figure 4 shows a typical reaction rate profile in the CTO. As soon as oxygen was introduced into the flow, oxidation started with a peak and the oxidation rate decreased with gradual depletion of the remaining carbon.

Though carbon oxidation reaction is a heterogeneous reaction, it is known that the carbon-oxygen reaction follows well the Arrhenius equation. The reaction constants can be derived from the following equations.

$$\frac{dm}{dt}=m^{n_C}\,k(T)P_{O_2}^{n_{O_2}} \quad (2)$$

$$k(T)=Ae^{\left(\frac{-E_a}{RT}\right)} \quad (3)$$

$$\ln(k)=\ln(A)-E_a/RT \quad (4)$$

$$\ln\left(\frac{dm}{dt}\right)=n_c\ln(m)+\ln(k(T)P_{O_2}^{n_{O_2}}) \quad (5)$$

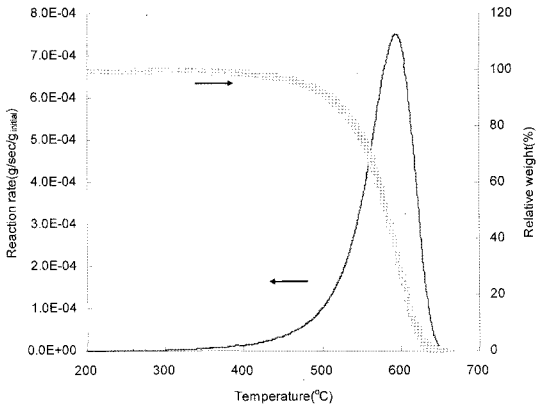

Figure 3. Reaction rate as a function of temperature, 3.8°C/min, O_2 10%.

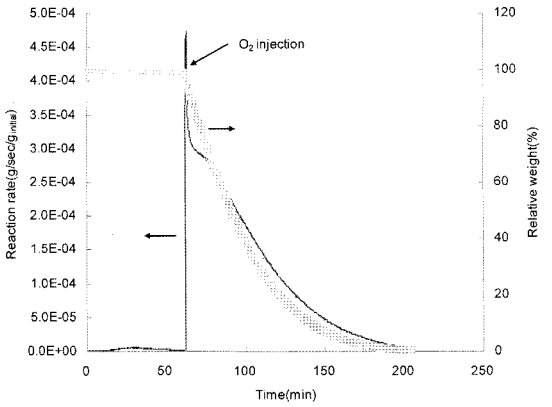

Figure 4. Reaction rate at constant temperature of 545°C, O_2 10%.

where
m : the sample soot mass undergoing reaction
n_C, n_{O2} : reaction order of carbon, oxygen
P_{O2} : oxygen partial pressure
k : specific reaction rate constant
E_a : activation energy
R : molar gas constant
T : temperature (K)

Specific reaction rate (k) is the reaction rate per nth-order of the remaining mass. If soot has a figure of perfect sphere and oxidation takes place only on the surface, the reaction order of the sample mass is 2/3 as in a shrinking core model. Reaction order for the carbon mass can be determined by Equation (5) from CTO result.

Figure 5 is the fit of Equation (5) in CTO (at 522, 545, 567°C). The slope indicates the reaction order for the carbon mass. After 35–40% conversion of the initial carbon amount, the reaction order for the carbon mass was found to be nearly constant (0.8 ± 0.02, $R^2 > 0.999$) at the different temperatures, which implies that the

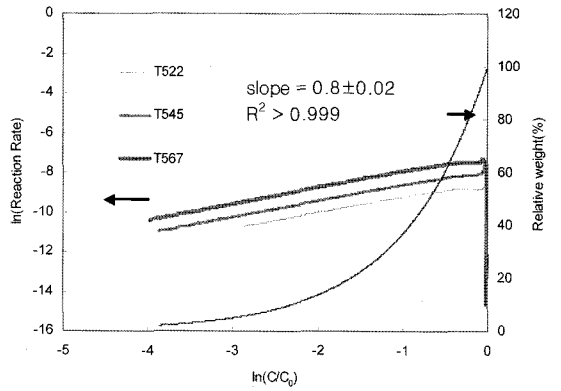

Figure 5. Fit of Equation (5). Reaction order is equal to the slope. O_2 10%, in CTO (522°C, 545°C, 567°C).

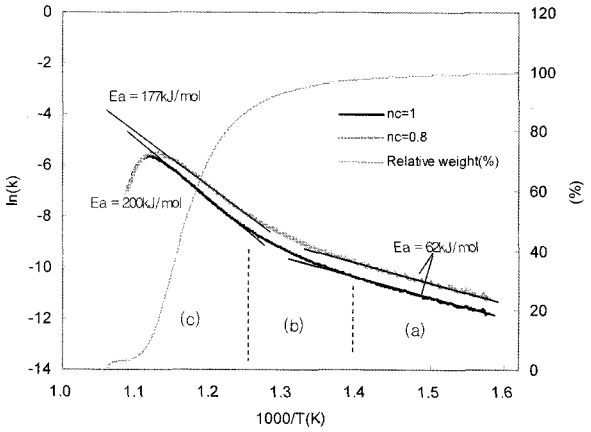

Figure 6. Arrehnius plot of the TPO with different reaction orders, O_2 10%.

oxidation kinetics is dominated by one reaction in this conversion and temperature range. In the earlier stage of conversion, the reaction order was difficult to be determined.

Figure 6 is the Arrehnius plot of the TPO result. It shows two apparent linear slopes in the lower temperature or early period of the oxidation (a) and the higher temperature or later period of the oxidation (c). The period (a) occupies 3–4% of total conversion. The period (c) of 25% to 80–90% conversion has another linear fit. Therefore it can be assumed that after some amount of the initial carbon is oxidized the state of carbon to oxidation does not change in both CTO and TPO conditions.

It has been known that carbon oxidation takes place through the formation of surface oxygen complexes (SOCs), which play an essential role in the carbon oxidation mechanism. They react as initial part of the soot particle as well as intermediates in the oxidation process. Oxygen in soot exists as the form of oxidized carbon. It has been shown by DRIFT (diffuse reflectance infrared Fourier transformed) analysis that SOCs can exist as quinone, anhydride, carbonyl, lactone, carboxylic, etc. (Setiabudi *et al.*, 2004). Considering carbon oxidation occurs at the active sites on the outer surface, total carbon (C_{tot}) can be specified into inner carbon part (C), carbon with active site (C^*), and carbon with active site occupied by oxygen (SOC, C*(O)). Then total carbon amount can be described by Equation (7).

$$C_{tot}=C+C^*+C^*(O) \tag{7}$$

On the assumption that the number of total active carbon site (C^*_{tot}) is proportional to the surface area, the total fraction of active carbon site can be expressed as Equation (8). Then Equation (7) can be rearranged as Equation (9).

$$C^*_{tot}=f_a \cdot (C_{tot})^{n_c} \tag{8}$$

$$C_{tot}=C+(1-\xi) \cdot C^*_{tot}+\xi \cdot C^*_{tot} \tag{9}$$

f_a is referred to the specific fraction of active site, which is related to its initial primary particle diameter, crystalline structure, and chemical status of the active sites, which can differ between carbon origins. ξ is referred to the fraction of active carbon site occupied by oxygen.

The active sites on the surface should be regenerated from the inner carbon beneath the surface through oxidation. We assumed that all the oxidation result in the formation of SOCs as well as CO or CO_2 production. In the CTO as shown in Figure 4 and 5 after 35–40% conversion the specific reaction rate in Equation (2) was constant. It implies that there was no change in the state of active sites in the conversion period. Consequently, it can be assumed that the active sites become saturated with oxygen (forming SOCs) as the oxidation proceeds. Then, with the inner carbon and the surface active carbon sites which are initially either occupied or unoccupied by oxygen as presented in Equation (7), a carbon oxidation mechanism can be suggested by the following reactions. Reaction {3} represents thermal desorption of SOCs. CO_x can be either CO or CO_2.

$$C+C^*+O_2 \xrightarrow{k_1} CO_x+C^*(O) \quad \{1\}$$

$$C+C^*(O)+O_2 \xrightarrow{k_2} CO_x+C^*(O) \quad \{2\}$$

$$C+C^*(O) \xrightarrow{k_3} CO_x+C^* \quad \{3\}$$

The reaction rates for total carbon is

$$\frac{dC_{tot}}{dt}=-k_1C^*P_{O_2}^{n_{O_2}}-k_2C^*(O)P_{O_2}^{n_{O_2}}-k_3C^*(O) \tag{10}$$

The total number of active sites is limited by Equation (8) and decreases as carbon particle shrinks by oxidation from the outer surface. As a result, the production of

$C^*(O)$ and C^* in Reaction {1}, {3}, and the regeneration of $C^*(O)$ in Reaction {2} cannot be the same amount for each consumption of the carbon at the active site. On the assumption that the fraction of SOCs in the active sites is maintained after each step of the reaction, then the evolution of the active sites can be defined as

$$\xi_i=\frac{C^*(O)_i}{C^*_{tot,i}} = \frac{C^*(O)_{i-1}+k_1 C^*(O)_{i-1} P_{O_2}^{n_{O_2}} dt - k_3 C^*(O)_{i-1} dt}{C^*_{tot,i-1}} \quad (13)$$

$$C^*_i = C^*_{tot,i} - C^*(O)_i \quad (14)$$

The each reaction coefficients in Reaction {1}–{3} was determined empirically from TPO and CTO by comparing Arrehnius plots and reaction rates between the experimental results and the simulation with the presented reaction mechanism.

By assuming most of the oxygen in carbon exists on the surface, and simplifying all the SOCs as a form of C-O, the relation between the amount of SOCs and the oxygen weight fraction can be approximated by Equation (15). M_w is the atomic weight.

$$O(wt\%)=\left(\frac{x\cdot C^*(O)}{C_{tot}+x\cdot C^*(O)}\right)\times 100 \quad x=\frac{M_{w,O}}{M_{w,C}} \quad (15)$$

The specific fraction of active sites was determined from the experimental result. From Figures 4 and 5, the surface active carbon site can be supposed to be fully saturated with oxygen (ξ=1, $C^*_{tot} = C^*(O)_{tot}$) after 40% of conversion in CTO. An experiment was made to evaluate the saturated amount of SOCs. With the same condition of the CTO in Figure 4, at the moment of 40% of conversion, oxygen supply was replaced with nitrogen and temperature was cooled down quickly to under 100°C. Then the temperature was increased up to 900°C to desorb SOCs thermally by Reaction {3}. By integrating the CO_x emissions, the total amount of SOCs was evaluated to be 12.5% to the total remaining carbon. Then, from Equation (8), f_a was determined to be 0.2 by substituting C_{tot} with 60% of the initial carbon mass and C^*_{tot} with 12.5% of C_{tot}. In this thermal desorption procedure, the activation energy and the frequency factor of the Reaction {3} were also determined.

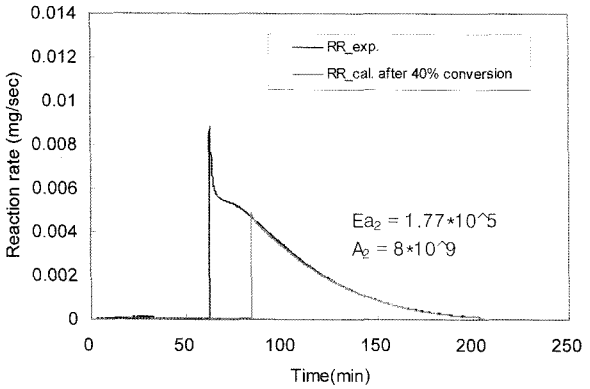

Figure 7. Adjustment of the frequency factor of reaction {2}. O_2 10%, 545°C.

Table 2. Reaction rate coefficients of the reaction scheme.

Reaction #	1	2	3
Ea (kJ/mol)	60±1	177±0.5	37±1
A	1.20×10^2	8×10^9	3.0×10^{-2}

*n_C: 0.8, n_{O_2}: 1.0

With the initial condition of the 60% remaining carbon saturated with SOCs, the frequency factor of the Reaction {2} can be determined by curve fitting of the calculated reaction rate of the CTO as shown in Figure 7.

The initial fraction of SOC (ξ_0) was determined to be 0.2 by Equation (8), (9), (15) with the initial oxygen fraction in Table 1. The reaction constants of the Reaction {1} cannot be determined individually like the case of Reaction {2} and {3} due to the effect of Reaction {3}. It can be derived from the Arrehnius plot of TPO simulation.

The Reaction rate constants from the presented reaction scheme and the experimental data are shown in Table 2.

Figure 8 shows the Arrehnius plots of the TPO and the simulation by the presented reaction scheme. The experimental data and the simulation result correlated well with each other up to 90% conversion.

Figure 9 and 10 compares the experimental data and the simulation in CTO. The initial high reactivity was not simulated, while the rest over 90% conversion period is in good accordance. Yezerets *et al.* (2003) observed that this initial high reactivity is not due to the additional

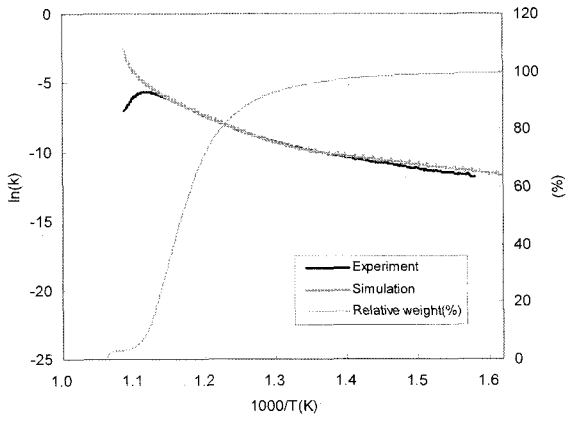

Figure 8. Arrhnius plot of experiment and simulation in the TPO. O_2 10%.

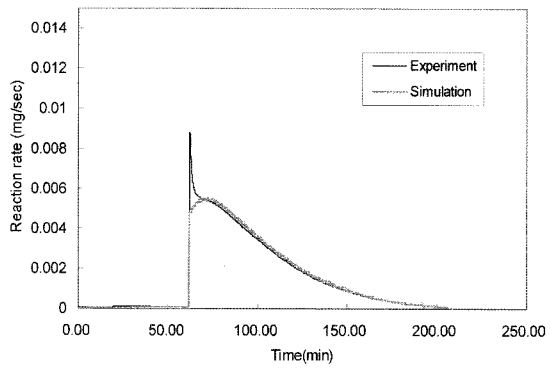

Figure 9. Reaction rate of CTO and simulation with the presented reaction mechanism. O_2 10%, 545°C.

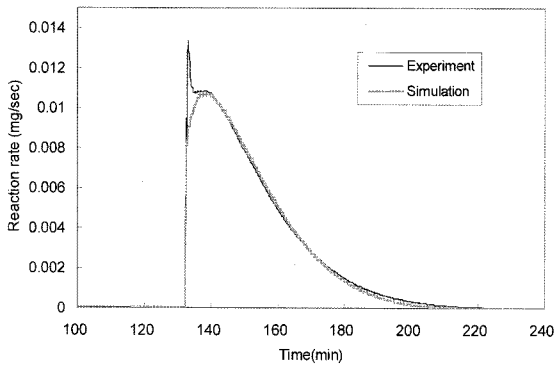

Figure 10. Reaction rate of CTO and simulation with the presented reaction mechanism. O_2 10%, 567°C.

component in soot such as adsorbed hydrocarbons, and it can be regenerated by the high temperature heat treatment in an inert gas or prolonged aging in the atmosphere. Therefore, it can be suggested that free active sites which is not occupied by oxygen might be responsible for this reactivity.

Further research is needed to simulate all the reaction rate evolution including the initial high reactivity.

4. CONCLUSION

We investigated soot oxidation characteristics with commercial carbon black of Printex-U as model soot in the flow reactor designed to simulate diesel particulate filter conditions and presented a simple reaction scheme from the empirical oxidation rate data.

From the temperature programmed oxidation two apparent activation energies were found. In the early stage of oxidation till 5% conversion the activation energy was much lower than that of the later stage of oxidation over 25% conversion. In the constant temperature oxidation the oxidation proceeds steadily after 40% conversion with the reaction order of carbon 0.8. The higher activation energy that covers most of the conversion range was 177±0.5 kJ/mol with the reaction order of 0.8, while 200 kJ/mol with 1st order for the carbon sample mass. From the two apparent activation energies and the reaction rate evolution in constant temperature oxidation, we proposed three reactions which correlate with experimental data on the assumption that the number of surface active sites is proportional to the surface area which is determined from carbon mass and reaction order of it. The proposed reaction scheme simulated the oxidation rate well in the experimented conditions over 90% of conversion range except the initial high peak of oxidation rate.

ACKNOWLEDGEMENT–This work is part of the project 'Development of Partial Zero Emission Technology for Future Vehicle' and we are grateful for its financial supportype.

REFERENCES

Allansson, R., Blakeman, P. G., Cooper, B. J., Hess, H., Silcock, P. J. and Walker, A. P. (2002). Optimising the low temperature performance and regeneration efficiency of the continuously regenerating diesel particulate filter (CR-DPF) system. *SAE Paper No.* 2002-01-0428.

Bokova, M. N., Decarne, C., Abi-Aad, E., Pryakhin, A. N., Lunin, V. V. and Aboukais, A. (2004). Kinetics of catalytic carbon black oxidation. *Thermochimica ACTA*, **428,** 165–171.

Clague, A. D. H., Donnet, J. B., Wang, T. K. and Peng, J. C. M. (1999). A comparison of diesel engine soot with carbon black. *Carbon,* **37,** 1553–1565.

Dieselnet Technology Guide (2005). *Diesel Particulate Filters.* www.dieselnet.com

Gilot, P., Nonnefoy, F., Marcuccilli, F. and Prado, G. (1993). Determination of kinetic data for soot oxidation. Modeling of competition between oxygen diffusion and reaction during thermogravimetric analysis. *Combustion and Flame,* **95,** 87–100.

Haralampous, O. A., Kandylas, I. P., Koltsakis, G. C. and Samaras, Z. C. (2004). Experimental evaluation of apparent soot oxidation rates in diesel particulate filters. *Int. J. Vehicle Design* **35, 4,** 365–382.

Jung, H., Kittelson, D. B. and Zachariah, M. R., (2004). Kinetics and visualization of soot oxidation using transmission electron microscopy. *Combustion and Flame,* **136,** 445–456.

Neeft, J. P. A., Hoornaert, F., Makkee, M. and Moulijn, J. A. (1996). The effects of heat and mass transfer in thermogravimetrical analysis. A case study towards the catalytic oxidation of soot. *Thermochimica ACTA,* 261–278.

Setiabudi, A., Makkee, M. and Moulijn, J. A. (2004). The

role of NO_2 and O_2 in the accelerated combustion of soot in diesel exhaust gases. *Applied Catalysis B: Environmental,* **50,** 185–194.

Stanmore, B. R., Brilhac, J. F. and Gilot, P. (2001). The oxidation of soot: a review of experiments. mechanisms and models. *Carbon,* **39,** 2247–2268.

Su, D. S., Jentoft, R. E., Muller, J.-O., Rothe, D., Jacob, E., Sompson, C. D., Tomovic, Z., Mullen, K., Messerer, A., Poschal, U., Niessner, R. and Schologl, R. (2004). Microstructure and oxidation behaviour of Euro IV diesel engine soot: a comparative study with synthetic model soot substances. *Catalysis Today,* **90,** 127–132.

Stratakis, G. A. and Stamatelos, A. M. (2003). Thermogravimetric analysis of soot emitted by a modern diesel engine run on catalyst-doped fuel. *Combustion and Flame,* **132,** 157–169.

Vander Wal, R. L. and Tomasek, A. J. (2003). Soot oxidation: dependence upon initial nasostructure. *Combustion and Flame*, **134,** 1–9.

Vincent, M. W, Rechards, P. J. and Rogers, T. J. (2002). Effective particulates reduction in diesel engines through the use of fuel catalysed particulate filters. *Int. J. Automotive Technology* **3, 1,** 1–8.

Yezerets, A., Currier, N. W., Eadler, H., Popuri, H. and Suresh, A. (2002). Quantitative flow-reactor study of diesel soot oxidation process. *SAE Paper No.* 2002-01-1684.

Yezerets, A., Currier, N. W., Eadler, H. A., Suresh, A., Madden, P. F. and Branigin, M. A. (2003). Investigation of the oxidation behavior of diesel particulate matter. *Catalysis Today,* **88,** 17–25.